ChemComm

Accepted Manuscript

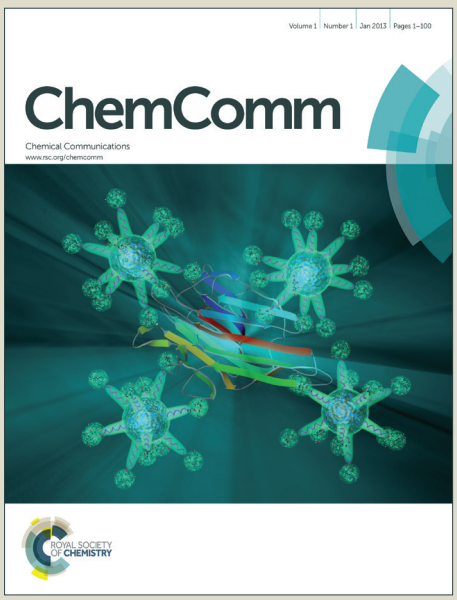

ROYAL SOCIETY OF CHEMISTRY

www.rsc.org/chemcomm

Journal Name

RSCPublishing

COMMUNICATION

Photo-Induced Charge Recombination Kinetics in $MAPbI_{3-x}Cl_x$ Perovskite-like Solar Cells Using Low Band-Gap Polymers as Hole Conductors.

Cite this: DOI: 10.1039/xoxxoooooox

Received ooth January 2012,
Accepted ooth January 2012

DOI: 10.1039/xoxxoooooox

www.rsc.org/

Jose Manuel Marin-Beloqui,[a] Javier Pérez Hernández,[a] Emilio Palomares*[a,b]

We measured the charge recombination kinetics using Transient Photovoltage (TPV) and Laser Transient Absorption Spectroscopy (L-TAS) in $MAPbI_{3-x}Cl_x$ perovskite solar cells using low band gap polymers as hole transport materials (HTM). Unequivocally, we assigned both transient decays to the recombination process between photo-injected electrons at the TiO_2 and the oxidised polymers.

Hybrid inorganic/organic double heterojunction solar cells have been the focus of intense research mainly to replace the liquid red/ox electrolyte in mesoscopic TiO_2 dye sensitized solar cells (DSSC)[1]. In most cases, the same sensitizer is used for both architectures but the liquid electrolyte is replaced by a solution process hole transport material (HTM), generally either the spiro-OMeTAD[2] (chemical name: 2,2',7,7'-tetrakis(N,N-di-p-methoxyphenylamine) or a semiconductor polymer such as P3HT (chemical name: Poly(3-hexylthiophene)[3]. However, the light-to-energy conversion efficiency (η) of these, so called, solid-state DSSCs have been generally below the efficiency values of their liquid counterparts mainly due to the lower photocurrent produced in the thinner mesoporous TiO_2 layers needed for solid-state DSSCs or the desorption of the sensitizer after the spin-coating of the HTM which frequently requires organic solvents such as chlorobenzene.

A breakthrough in the double heterojunction was reported in 2013 by several research groups[4] working independently by replacing the sensitizer using an organolead halide, either $CH_3NH_3PbI_3$ or $CH_3NH_3PbI_{3-x}Cl_x$ ($MAPbI_3$ or $MAPbI_{3-x}Cl_x$), and using spiro-OMeTAD as the hole conductor with outstanding efficiencies surpassing 15% under standard measurement conditions.

These results fuelled the interest of many research groups devoted to the study of DSSC and OSC (organic solar cells) and many different device configurations have been studied with published efficiencies ranging from 10% for thin-film approaches that avoid the use of HTM (see **Scheme 1**) to over 16% for those device structures that use HTM.

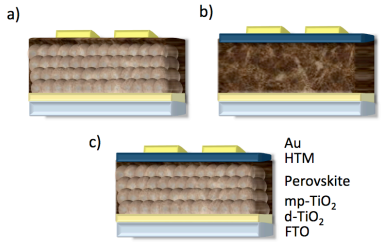

Scheme 1. Different device structures for MAPbI or MAPbICl based solar cells. (a) Thin-film approach without the use of a HTM. (b) Thin-film approach without the use of mp-TiO_2 and (c) the meso-structured approach using both mp-TiO_2 and HTM.

Most studies have focussed on replacing the spiro-OMeTAD HTM material with alternative HTM molecules with great success but studies on the photo-induced interfacial charge recombination reactions in these novel solar cells are more scarce[5]. However, the study of the charge recombination processes under operation conditions are paramount to advance towards the theoretical maximum efficiency of $MAPbI_{3-x}Cl_x$ solar cells[6] by minimizing the interfacial losses, as for example the charge recombination reaction between the photo-injected electrons at the TiO_2 and the oxidised HTM (reaction 3 in **Scheme 2**).

In this communication we have fabricated efficient mp-TiO_2/$MAPbI_{3-x}Cl_x$ devices using as HTM materials two semiconductor low-band gap polymers, PTB1 and PTB7, that show excellent hole mobility in OPV devices ($4.5\ 10^{-4}$ $cm^2V^{-1}S^{-1}$ and $5.8\ 10^{-4}$ $cm^2V^{-1}s^{-1}$ for PTB1 and PTB7 respectively).

Figure 1 shows the IV curves for both type of solar cells and the standard solar cell using spiro-OMeTAD for comparison purposes.

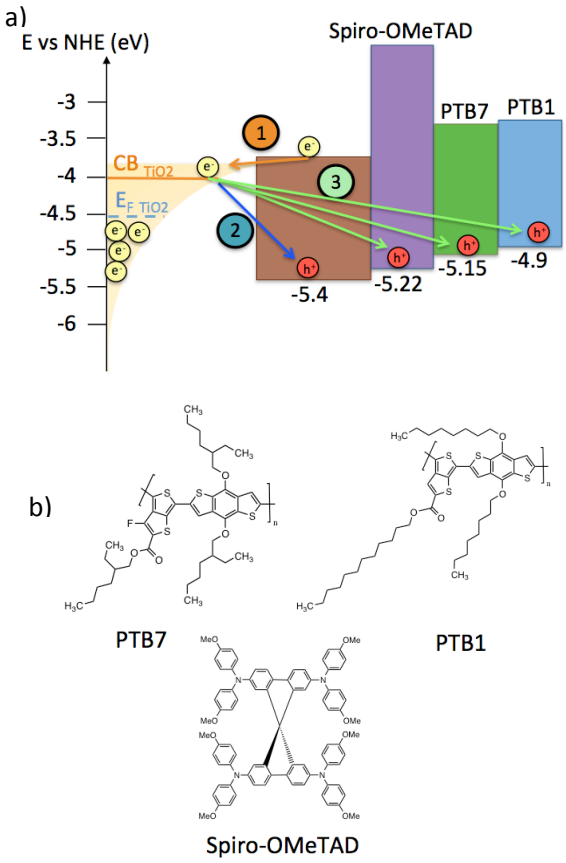

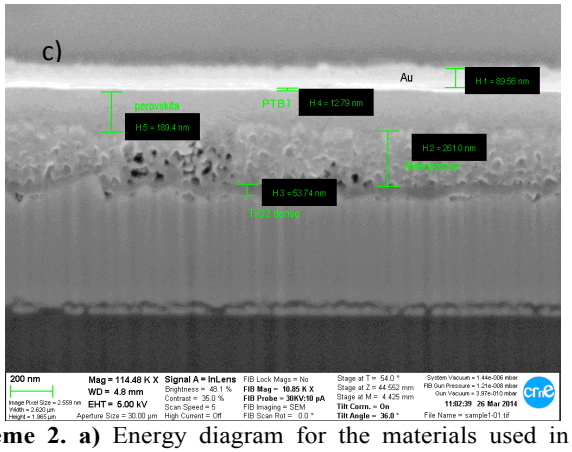

Scheme 2. a) Energy diagram for the materials used in our devices (energy numbers in eV). The arrows correspond to the interfacial charge transfer reactions occurring during working conditions: (1) charge injection, (2) charge recombination between the photo-injected electrons in the TiO_2 and the holes in the perovskite material, (3) as in (2) but the recombination reaction occurs with the oxidised HTM. **b)** Molecular structure of the HTM materials used in our study. **c)** High resolution scanning electron microscopy image of the sections of our PTB1 based solar cell. H1= Gold contact (thickness: 89.6nm), H2=mp-TiO_2 (thickness: 261.0nm), H3=d-TiO_2 (thickness: 53.7nm), H4= PTB1 (thickness: 12.8nm), H5= perovskite (thickness: 189.4nm).

To simplify our discussion the use of chemical additives such as 1,8 di-iodooctane (DIO), 4-tert-Butyl Pyridine (tBuPyr) or Lithium Bis(Trifluoromethanesulfonyl)Imide (LiTFSI) on the semiconductor polymers was avoided. Nonetheless, efficiencies as high as the ones reported for other semiconductor polymers in similar device structures have been achieved as listed in **Table 1**.

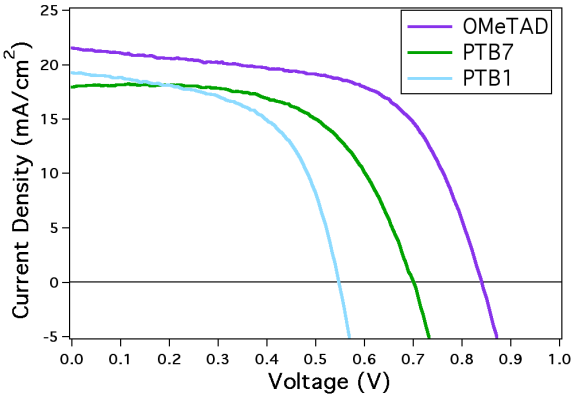

Figure 1. Photocurrent vs voltage (IV curves) measured at 1 sun (100mW/cm^2 1.5 AM G sun-simulated light) for our best devices using the different HTMs.

Table 1. IV curve parameters for our best devices.

HTM	Jsc (mA/cm^2)	Voc (mV)	FF (%)	PCE, η (%)
Spiro-OMeTAD	21.6	839	60.5	10.9
PTB1	19.3	543	57.2	6.0
PTB7	18.0	699	59.8	7.5
PCPDTBT	10.3	770	66.7	5.3*
PCDTBT	10.5	920	43.7	4.2*

Jsc= Device short-circuit photocurrent density. Voc= Open circuit photovoltage. FF = Fill factor. PCE, η= Solar cell efficiency.* From Reference 7[7].

It is important to note that the devices were stable during the time necessary to characterize the recombination kinetics using TPV and L-TAS as shown in the ESI.

The devices were fabricated using a 50 nm thick layer of dense TiO_2 (d-TiO_2) and a 300 nm thick mesoporous TiO_2 (mp-TiO_2) layer all deposited onto FTO (fluorine doped Tin Oxide) glass with a resistance of 8Ω/cm^2 following previous literature. The $CH_3NH_3PbI_{3-x}Cl_x$ was afterwards deposited on the mp-TiO_2 spin-coating a $PbCl_2$:CH_3NH_3I solution in DMF with a molar ratio of 1:3. The deposition of the metal oxide layers were carried out under ambient conditions but the subsequent deposition of the $MAPbI_{3-x}Cl_x$ was carried out in a glove box ([H_2O] < 0.1 ppm and [O_2] < 100 ppm content). Each semiconductor polymer was spin-coated onto the FTO/d-TiO_2/mp-TiO_2/$MAPbI_{3-x}Cl_x$ at 2000rpm for 60 s from a solution of chlorobenzene (10 mg/mL). The devices made using spiro-OMeTAD as HTM were fabricated using an identical protocol. **Scheme 2c** shows the cross-sectional scanning electron microscopy image for a PTB1 device. **Figure 2** shows the different L-TAS transient decays for the films upon excitation using our nanosecond Nd-YAG laser system (see ESI).

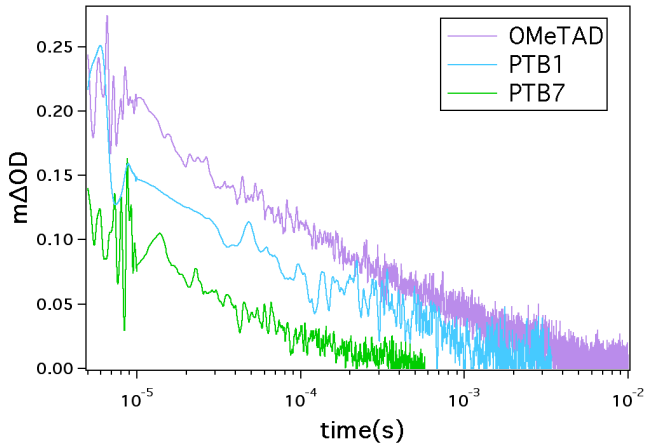

Figure 2. L-TAS decays, under ambient conditions, for the FTO/d-TiO_2/mp-TiO_2/$MAPbI_{3-x}Cl_x$/HTM films exciting at λ_{ex}=500nm for the spiro-OMeTAD films and λ_{ex}=700m for both semiconductor polymer films. The probe wavelengths were λ_{pr}=1400nm for the spiro-OMeTAD, λ_{pr}= 1100nm for the PTB7 and λ_{pr}= 980nm for the PTB1 films.

As can be seen, the signal amplitude for the spiro-OMeTAD and the PTB1 films are greater than that for the PTB7 film and, moreover, the decay lifetime for the spiro-OMeTAD is also slower, which implies that the back-electron transfer from the photo-injected electrons in the TiO_2 to the oxidised spiro-OMeTAD (reaction 3 in **Scheme 2**) is much slower than for the polymers. This can help explain why spiro-OMeTAD based devices are more efficient. We could estimate qualitatively the efficiency on the regeneration of the perovskite ground state from these signal amplitudes. However, the unknown molar absorption coefficient of the HTM^+ polarons for both spiro-OMeTAD and the semiconductor polymers makes it difficult to ensure that the larger signal amplitude for spiro-OMeTAD corresponds to a better regeneration of the pervoskite ground state. Further work is in progress regarding this. Nonetheless, additional data using Time Correlated Single Photon Counting (TCSPC) (see ESI) shows differences in luminescence quenching of the perovskite for the different HTM materials in perfect agreement with the L-TAS signal amplitude.

In order to validate our hypothesis that the L-TAS signal corresponds to the recombination between the photo-injected electrons and the oxidised HTM, we carried out TPV measurements in complete devices and compare the TPV decay with the L-TAS decay (**Figure 3**). This assumption cannot be done without the combination of both time-resolved techniques.

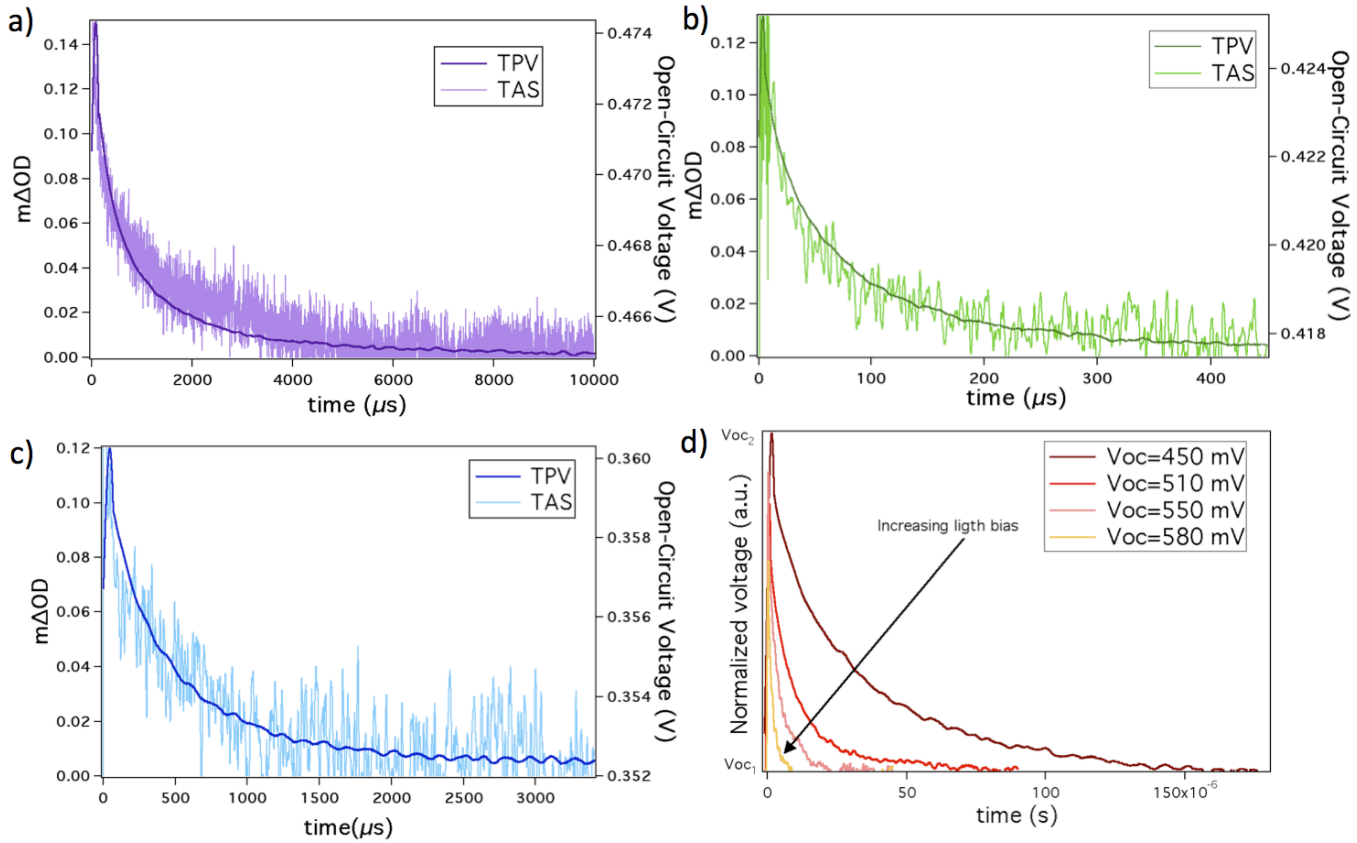

Figure 3. TPV and L-TAS decays measured for the different devices. Notice the different Voc (right Y axis) for the different devices. (a) Spiro-OMeTAD, (b) PTB7, (c) PTB1 and (d) different TPV decays at different light bias (solar cell photovoltage at different light intensities) for the PTB1 device.

TPV is a technique that allows the measurement of the photo-induced recombination kinetics in complete devices under device working conditions[8]. Upon light illumination the solar cells generate a photovoltage (Voc_1) that can be perturbed using a fast-pulsed laser. Upon excitation it generates a small increment of charges injected from the organolead halide to the

TiO_2 raising the photovoltage to Voc_2. This increase in Voc, ΔV, is proportional to the raise in the Fermi level of the TiO_2. After the laser pulse, the original Voc_1 is restored with a lifetime (τ) that is the time that it takes the excess photoinjected charges (resulting from the laser pulse) to recombine and return the solar cell to the initial photovoltage Voc_1. It is important to note that the laser pulse must be small in energy ($\Delta V<15mV$) to obtain a mono-exponential decay. **Figure 3** shows the TPV decays for the devices studied in this work.

As can be seen, the TPV and L-TAS decays fit in good agreement implying that, indeed, in both cases the charge transfer reaction measured corresponds unequivocally to the recombination reaction between the photo-injected electrons, from the $MAPbI_{3-x}Cl_x$ to the oxidised HTM^+. Moreover, as shown in **Figure 3d**, the increase of the light intensity (higher Voc) leads to faster TPV decays (faster charge recombination), which implies a direct relationship between increasing the charge density, increasing the solar cell Voc and faster recombination kinetics between the photo-injected electrons at the TiO_2 and the oxidised materials used as HTM.

Conclusions

We have fabricated efficient solar cells using $MAPbI_{3-x}Cl_x$ as the light harvesting material and low band gap semiconductor polymers such as PTB1 and PTB7 as HTM. The interfacial charge transfer dynamics were probed using micro-second to millisecond L-TAS. The L-TAS signals suggest better regeneration kinetics for the spiro-OMeTAD and the PTB1 polymer in complete $MAPbI_{3-x}Cl_x$ solar cells. Moreover, the L-TAS kinetics appear slower for the spiro-OMeTAD films. To confirm our hypothesis we measured TPV in complete devices, at different light bias, and we found that for low light intensities, close to the ones used in our L-TAS experiments, the TPV and L-TAS decays fit in perfect agreement. The increase of the light intensity leads to higher device Voc with faster TPV decays in all cases, suggesting that there is a direct correlation between photo-induced charge density, solar cell open circuit voltage (Voc) and faster recombination kinetics. Thus, in order to compare recombination kinetics in organolead halide based solar cells, it will be necessary to know beforehand the charge density in the devices under illumination as different device charge lifetime may well be due to the different charge density at the solar cell.

Acknowledgments.
The authors would like to thank the Spanish MICINN for financial support (projects CTQ-2010-18859 and CTQ-2013-47183R). EP also thanks the ERC for the PolyDot funded project.

Notes and references

[a] Institute of Chemical Research of Catalonia (ICIQ). Avda. Països Catalans, 16. Tarragona. E-43007. Spain
[b] Catalan Institution for Research and Advanced Studies (ICREA). Passeig Lluís Comanys, 23. Barcelona. E-08010. Spain.

Electronic Supplementary Information (ESI) available: Experimental section for device preparation. The double heterojunction scheme, the stability IV curve measurement as well as the description of the systems used to acquire the data using L-TAS, TPV and TCSPC.
See DOI: 10.1039/c000000x/

REFERENCES

1. B. Li, L. Wang, B. Kang, P. Wang and Y. Qiu, *Sol. Energ. Mat. Sol.*, 2006, **90**, 549-573.
2 H. J. Snaith and L. Schmidt-Mende, *Adv. Mat.*, 2007, **19**, 3187-3200.
3 (a) L. Yang, U. B. Cappel, E. L. Unger, M. Karlsson, K. M. Karlsson, E. Gabrielsson, L. Sun, G. Boschloo, A. Hagfeldt and E. M. J. Johansson, *Phys. Chem. Chem. Phys.*, 2012, **14**, 779-789; (b) F. Freitas, J. Clifford, E. Palomares and A. Nogueira, *Phys. Chem. Chem. Phys*, 2012, **14**, 11990-11993
4 (a) M. M. Lee, J. l. Teuscher, T. Miyasaka, T. N. Murakami and H. J. Snaith, *Science*, 2012, **338**, 643-647; (b) G. Xing, N. Mathews, S. Sun, S. S. Lim, Y. M. Lam, M. Grätzel, S. Mhaisalkar and T. C. Sum, *Science*, 2013, **342**, 344-347; (c) J. Burschka, N. Pellet, S.-J. Moon, R. Humphry-Baker, P. Gao, M. K. Nazeeruddin and M. Gratzel, *Nature*, 2013, **499**, 316-319; (d) S. Ryu, J. H. Noh, N. J. Jeon, Y. Chan Kim, W. S. Yang, J. Seo and S. I. Seok, *Energ. Environ. Sci.*, 2014, **7**, 2614-2618; (e) J. You, Z. Hong, Y. Yang, Q. Chen, M. Cai, T.-B. Song, C.-C. Chen, S. Lu, Y. Liu and H. Zhou, *ACS Nano*, 2014, **8**, 1674-1680.
5 (a) S. Lv, L. Han, J. Xiao, L. Zhu, J. Shi, H. Wei, Y. Xu, J. Dong, X. Xu, D. Li, S. Wang, Y. Luo, Q. Meng and X. Li, *Chem. Comm.*, 2014, **50**, 6931-6934; (b) N. J. Jeon, J. Lee, J. H. Noh, M. K. Nazeeruddin, M. Grätzel and S. I. Seok, *J. Am. Chem. Soc.*, 2013, **135**, 19087-19090.
6 V. Gonzalez-Pedro, E. J. Juarez-Perez, W.-S. Arsyad, E. M. Barea, F. Fabregat-Santiago, I. Mora-Sero and J. Bisquert, *Nano Lett.*, 2014, **14**, 888-893.
7 J. H. Heo, S. H. Im, J. H. Noh, T. N. Mandal, C.-S. Lim, J. A. Chang, Y. H. Lee, H.-j. Kim, A. Sarkar, K. NazeeruddinMd, M. Gratzel and S. I. Seok, *Nat. Phot.*, 2013, **7**, 486-491.
8 (a) D. Joly, L. Pellejà, S. Narbey, F. Oswald, J. Chiron, J. N. Clifford, E. Palomares and R. Demadrille, *Scientific reports*, 2014, **4:4033**, 1-7; (b) A. Reynal, A. Forneli, E. Martinez-Ferrero, A. Sanchez-Diaz, A. Vidal-Ferran, B. C. O'Regan and E. Palomares, *J. Am. Chem. Soc.*, 2008, **130**, 13558-13567.

